Hydrologic Connectivity: Quantitative Assessments of Hydrologic-Enforced Drainage Structures in an Elevation Model

Authors: Poppenga, Sandra K., and Worstell, Bruce B.

Source: Journal of Coastal Research, 76(sp1) : 90-106

Published By: Coastal Education and Research Foundation

URL: https://doi.org/10.2112/SI76-009

Journal of Coastal Research	SI	76	90–106	Coconut Creek, Florida	2016

Hydrologic Connectivity: Quantitative Assessments of Hydrologic-Enforced Drainage Structures in an Elevation Model

Sandra K. Poppenga[†*] and Bruce B. Worstell[‡]

[†]U.S. Geological Survey
Earth Resources Observation and Science (EROS) Center
Sioux Falls, SD 57198, U.S.A.

[‡]Stinger Ghaffarian Technologies, Inc.
U.S. Geological Survey
Earth Resources Observation and Science (EROS) Center
Sioux Falls, SD 57198, U.S.A.

www.cerf-jcr.org

www.JCRonline.org

ABSTRACT

Poppenga, S.K. and Worstell, B.B., 2016. Hydrologic connectivity: Quantitative assessments of hydrologic-enforced drainage structures in an elevation model. *In*: Brock, J.C.; Gesch, D.B.; Parrish, C.E.; Rogers, J.N., and Wright, C.W. (eds.), *Advances in Topobathymetric Mapping, Models, and Applications. Journal of Coastal Research*, Special Issue, No. 76, pp. 90–106. Coconut Creek (Florida), ISSN 0749-0208.

Elevation data derived from light detection and ranging present challenges for hydrologic modeling as the elevation surface includes bridge decks and elevated road features overlaying culvert drainage structures. In reality, water is carried through these structures; however, in the elevation surface these features impede modeled overland surface flow. Thus, a hydrologically-enforced elevation surface is needed for hydrodynamic modeling. In the Delaware River Basin, hydrologic-enforcement techniques were used to modify elevations to simulate how constructed drainage structures allow overland surface flow. By calculating residuals between unfilled and filled elevation surfaces, artificially pooled depressions that formed upstream of constructed drainage structure features were defined, and elevation values were adjusted by generating transects at the location of the drainage structures. An assessment of each hydrologically-enforced drainage structure was conducted using field-surveyed culvert and bridge coordinates obtained from numerous public agencies, but it was discovered the disparate drainage structure datasets were not comprehensive enough to assess all remotely located depressions in need of hydrologic-enforcement. Alternatively, orthoimagery was interpreted to define drainage structures near each depression, and these locations were used as reference points for a quantitative hydrologic-enforcement assessment. The orthoimagery-interpreted reference points resulted in a larger corresponding sample size than the assessment between hydrologic-enforced transects and field-surveyed data. This assessment demonstrates the viability of rules-based hydrologic-enforcement that is needed to achieve hydrologic connectivity, which is valuable for hydrodynamic models in sensitive coastal regions. Hydrologic-enforced elevation data are also essential for merging with topographic/bathymetric elevation data that extend over vulnerable urbanized areas and dynamic coastal regions.

ADDITIONAL INDEX WORDS: *Hydrologically-corrected DEM validation, hydrologically-corrected DEM assessments, depression draining, hydrodynamic modeling.*

INTRODUCTION

As the risk for hazardous events resulting from climate change escalates, there is a need to accurately identify and map hydrologic connectivity between inland surface flow and coastal waters impacted by natural disasters. Because of the increased need to mitigate associated risks to communities and ecosystems, land use planners, managers, and scientists increasingly rely on high-resolution light detection and ranging (lidar) elevation surfaces to define overland surface flow on the landscape. Lidar elevation surfaces contain highly detailed topographic information. Therefore, raised features, such as road grade, can cause modeled surface flow to become impounded, resulting in a loss of hydrologic connectivity in the lidar elevation surface. Without hydrologic connectivity in a lidar elevation surface, uncertainties may arise in storm surge, inundation, or sea-level rise predictions that rely upon high-resolution elevation data. Therefore, lidar elevation surfaces, or lidar digital elevation models (DEMs), need to be hydrologically-corrected, or hydrologically (hydro)-enforced, prior to using the data in hydrodynamic models.

The objective of this paper is to contrast two types of quantitative assessments conducted in New Jersey coastal watersheds to demonstrate the feasibility of using hydro-enforcement to achieve hydrologic connectivity in lidar elevation surfaces. A description is provided of the complexities that arise when using culvert/bridge datasets, collected by numerous public agencies, as reference points to validate hydro-enforcement. A justification is also provided describing the need for a second quantitative assessment that consists of image interpretation of aerial photographs to identify reference drainage. Both types of assessments were conducted on hydro-enforced lidar elevation surfaces generated using previously published semi-automated hydro-enforcement methods developed by the U.S. Geological Survey (USGS) (Poppenga *et al*., 2010; 2012). The objective of this paper is an ambitious approach for several reasons: 1) quantitative assessments on semi-automated hydro-enforcement methods are rarely published in the scientific literature; 2) culvert/bridge reference points are not as readily available, as reliable, or as

DOI: 10.2112/SI76-009 received 26 August 2014; accepted in revision 16 July 2015.
*Corresponding author: spoppenga@usgs.gov

comprehensive as elevation control points, and 3) culvert/bridge reference points are not available to validate hydro-enforcement of depressions that are not located near roads.

The Need for Hydrologic Connectivity in Lidar Elevation Surfaces

This section explains the importance of achieving hydrologic connectivity in lidar DEMs. It also describes hydrologic connectivity issues that have been addressed in the scientific literature, and the lack of reference points to validate hydro-enforcement results in drainage structure locations.

As the need for coastal mapping, monitoring, and change detection increases in response to inundation hazards that impact vulnerable coastal zones (Brock and Purkis, 2009; Burkett and Davidson, 2012; Buxton *et al.*, 2013; Gesch, 2009; Gesch, Gutierezz, and Gill, 2009; Stoker *et al.*, 2009; Turnipseed *et al.*, 2007), hydrologic connectivity in lidar DEMs has become essential for storm surge and sea-level rise hydrodynamic modeling (ARCADIS, 2011; Gesch, 2009; Gesch, 2013; Li *et al.*, 2009; MacDonald, 2012; NOAA, 2010; Poulter, Goodall, and Halpin, 2008; Poulter and Halpin, 2008; Sheets, Brenner, and Gilmer, 2012; Westerink *et al.*, 2008; Zhang *et al.*, 2011). Although lidar has become a commonly used technology for the collection of highly accurate elevation information (Buxton *et al.*, 2013; Poppenga *et al.*, 2010; Schmid, Hadley, and Wijekoon, 2011; Stoker, Harding, and Parrish, 2008; Webster and Forbes, 2006) that is used for hydrologic applications (Brock and Sallenger, 2001; Medeiros, 2012; Medeiros *et al.*, 2011; Poppenga *et al*., 2010; 2012; 2013), according to Barber and Shortridge (2005), a high-resolution, high-accuracy elevation dataset does not necessarily produce a highly reliable model of overland surface flow. Lidar DEMs capture elevated features, such as road fill overlaying culverts, that impact any standard surface hydrology model by impeding the representation of overland surface flow (Figure 1A) (Barber and Shortridge, 2005; Duke *et al.*, 2003; Maune *et al*., 2007; Poppenga *et al*., 2013; Poppenga *et al*., 2014a,b). These elevated road features were not as problematic in the past with lower resolution (~30-m) DEMs derived from topographic maps because the level of topographic detail was much lower than lidar DEMs.

In situ, water is carried through culverts; however, because they are located beneath elevated road features, culverts cannot be represented in a lidar (topographic) DEM. Unless hydro-corrected, or hydro-enforced, these road features, so finely detailed in available lidar DEMs, create hydrologic connectivity issues (Poppenga *et al.*, 2010; 2012; 2013; Webster and Stiff, 2008). Without modifications to the elevation surface, water flow would be functionally dammed by the raised topography, creating artificial pooling of depressions on the upstream side (Heidemann, 2012a; 2012b; 2014; Maune, 2007; Poppenga *et al*., 2010, 2014a). Therefore, a hydro-enforced lidar DEM representing hydrologically connected modeled surface flow is needed for hydrodynamic modeling (Figure 1B) (Heidemann, 2012a; Poppenga *et al.*, 2014a,b).

Some hydrologic connectivity has been addressed with visual identification of culverts and bridges because (lidar) DEMs did not account for these features (Webster and Forbes, 2006; Webster and Stiff, 2008). However, these techniques do not consider the time consuming visual identification and manual hydro-enforcement. Other methods superimpose ancillary line networks into DEMs, such as stream burning (Saunders, 2000) or culvert burning (Stiff, Hopkinson, and Webster, 2008), or adaptive drainage enforcement (Kenny and Matthews, 2005; Soille, Vogt, and Colombo, 2003; Turcotte *et al.*, 2001; Zhang and Huang, 2009). These approaches may result in alignment issues, especially in high-resolution (lidar) DEMs (Chow, 2010), and may alter the integrity of an elevation surface, especially in stream network locations (Poppenga *et al.*, 2013).

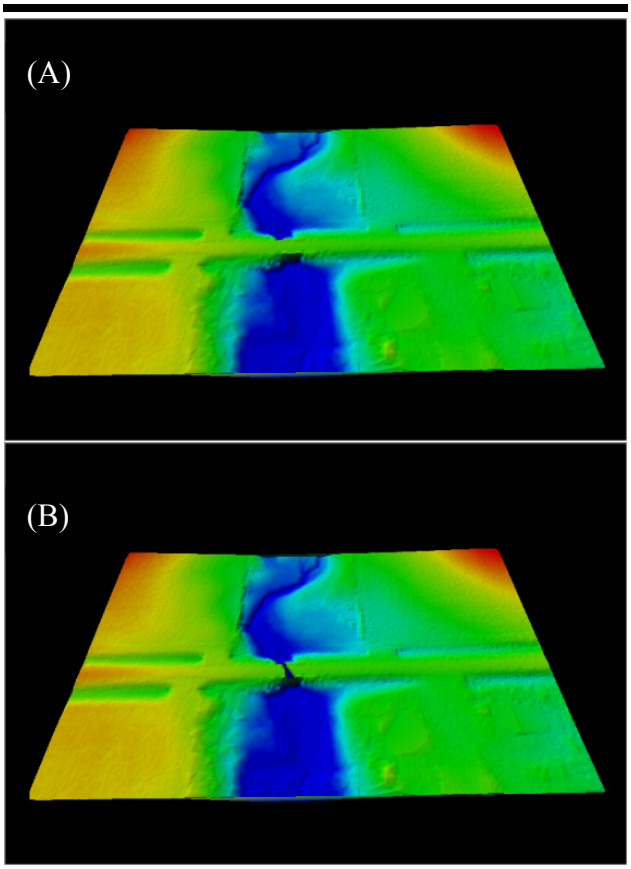

Figure 1. Topographic digital elevation model (DEM) representation of road surface elevation overlying a culvert (A). Hydrologic DEM representation showing hydrologic-enforcement at the culvert location (B).

Superimposing line networks does not address the extraction of fine-scale (2–5 m) stream channels (Cho *et al.*, 2011), which are not available as vectors (line networks). Additionally, raised surfaces with underlying drainage pipes are not always located along roads (Chow, 2010). Although Cho, Kampa, and Slatton (2007) demonstrated the feasibility of fine-scale stream extraction, they had difficulties connecting stream segments. Thus, a simple vector superimposition does not solve the hydrologic connectivity issue.

Alternatively, a method that can produce raster (grid) and vector (line) hydrologic connectivity is a digital hydro-enforcement approach as presented by Poppenga *et al.* (2010; 2012; 2013; 2014a,b). This approach uses residuals calculated between unfilled and filled lidar elevation surfaces to define artificially pooled depressions that form and are in need of hydro-enforcement. This method creates a hydrologically connected lidar DEM that models the flow of water across the land surface and consists of a suite of hydrologic derivatives that are consistently integrated with the high-resolution elevation data (Poppenga *et al.*, 2009). To determine the feasibility of this digital hydro-enforcement method, two different types of quantitative assessments were conducted. The goal of the first assessment was to use culvert and bridge datasets, collected by public agencies, to validate the hydro-enforcement. However, because of the lack of comprehensive culvert/bridge reference point datasets that can be used to conduct hydro-enforcement assessments (Chow, 2010), it was necessary to conduct a second assessment of image-interpreted culverts and bridges.

Hydrologic-Enforcement Quantitative Assessments

This section describes the paucity of reference points to validate hydro-enforcement, and the challenges that arise when conducting assessments on hydro-enforced drainage structure locations.

In the scientific literature, hydrologic uncertainty assessments have been presented, however, these studies pertain to rainfall, river discharge, or water quality (Heistermann and Kneis, 2011; McMillan, Krueger, and Freer, 2012; Seibert, 2001). A Hydrologic Benchmark Network was established by Leopold (1962), but at most this network contains 58 drainage basins in 39 states and was developed to provide long-term measurements of streamflow and water quality in areas virtually free of human activities (Mast and Turk, 1999; Murdoch *et al.*, 2005). Therefore, the challenge of hydro-enforcement validation originates from the lack of hydrologic benchmarks that can be referenced as ground truth (Chow, 2010). This problem is compounded by the paucity of hydro-enforcement accuracy assessments, which lag behind the ever-increasing demand for lidar-derived hydrologic information.

Hydro-enforcement validation is problematic because drainage structure reference points are not readily available or even as accurate as control points that are available for DEM accuracy assessments. Considering the lack of drainage structure reference points that contain as high of a degree of accuracy, frequency, and availability as the control points that are used for elevation assessments (Evans *et al.*, 2014; Gesch, Oimoen, and Evans., 2014; National Geodetic Survey, 2012; Samsung *et al.*, 2013; Thatcher *et al.*, 2014), conducting a hydro-enforcement assessment requires a creative approach.

Hydrologic studies are often conducted over relatively large regions using high-resolution lidar-based DEMs. Collecting survey-grade reference points for thousands of culverts and bridges in an attempt to conduct a hydro-enforcement assessment is not feasible during a project timeframe. Because an all-encompassing nationwide drainage structures database was not available, georeferenced coordinates for culverts and bridges were obtained from various public agencies. Combining these disparate field surveys into one dataset would seem to be a viable solution for obtaining an independent reference point dataset. However, collectively, these surveyed data are a medley of drainage structure types, geographic locations, and collection dates obtained using various mapping techniques with varying levels of positional accuracy.

Therefore, the challenge of hydro-enforcement assessments lies not only in obtaining the actual field survey datasets from public agencies but also in the lack of a comprehensive drainage structure dataset. Ancillary field survey collections will never be 100% of what is needed to assess hydro-enforcement because of the staggering amount of depressions that are created when hydro-conditioning (filling) a lidar DEM. Although many of the depressions are caused by noise and artifacts in the detailed lidar DEM, field-surveyed data cannot contain coordinates for every location that becomes impounded by elevated features other than road fill in the lidar DEM. Therefore, in this article, an approach is presented that encompasses two types of hydro-enforcement assessments in select watersheds in the Delaware River Basin.

METHODS

Four sections comprise the Methods part of this article. The Study Areas section describes three Delaware River watersheds in New Jersey and Pennsylvania where hydro-enforcement assessments were analyzed. The Data Sources section includes information about lidar data, ancillary drainage structures, and digital orthophoto quadrangles (DOQs) used in the quantitative assessments. The Hydrologic-Enforcement Methods section is an overview of previously published techniques on semi-automated procedures to hydro-enforce lidar DEMs (Poppenga *et al*., 2010; 2012). The Quantitative Assessments section describes the methods used to compare spatial correspondence between semi-automated hydro-enforcement and ancillary vector drainage structure data and DOQs.

Study Areas

An assessment was conducted of hydro-enforcement in Tinicum Creek, Lockatong Creek, and Jacobs Creek in the Delaware River Basin (Figure 2). These watersheds are part of the Newark Basin in Pennsylvania and New Jersey and consist of rural landscapes. The watersheds were selected because they are designated by the U.S. Department of the Interior as named tributaries included in the National Wild and Scenic Rivers System tributaries of the Lower Delaware River that drain into the coastal Delaware Bay (Delaware River Basin Commission, 2004; National Park Service, 2012). The landscape of each study site is both variable and representative of coastal watershed regions.

The first study area is located in the Tinicum Creek watershed in Bucks County, Pennsylvania (Figure 2B). Tinicum Creek surface waters flow generally from north to south through its upper two branches, Rapp and Beaver Creek, and flow northeastward to the Delaware River confluence. The watershed drains an elevation-derived area of 62.60 km^2 with a minimum elevation value of 29.25 m and a maximum elevation value of 256.57 m. The landscape consists of steep vertical cliffs exposed along the streambed and forests interspersed with cultivated crops in the higher elevations.

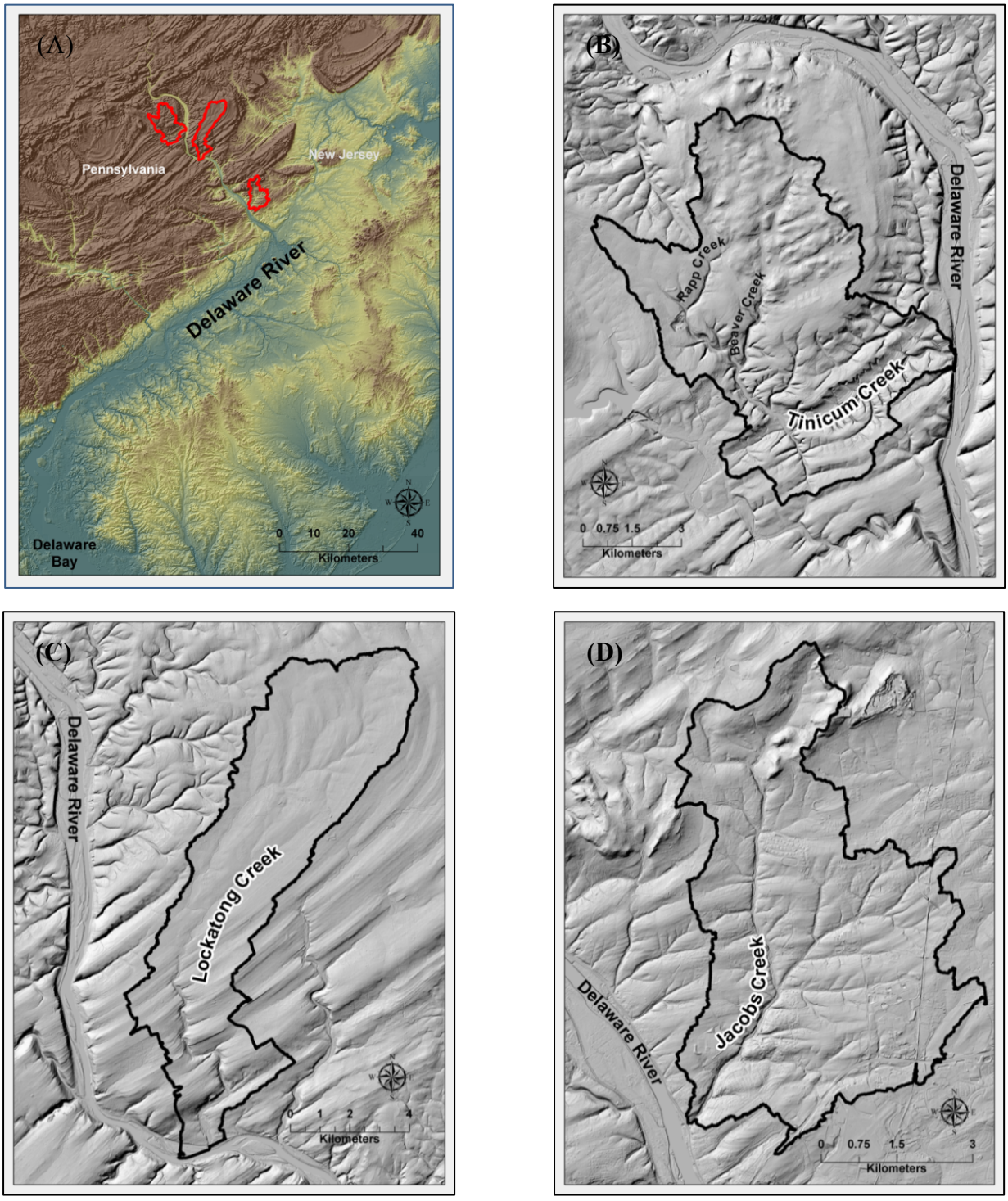

Figure 2. Lidar-derived watersheds in the Delaware River Basin study area (A). Tinicum Creek watershed, Bucks County, Pennsylvania (B). Lockatong Creek watershed, Hunterdon County, New Jersey (C). Jacobs Creek watershed, Mercer County, New Jersey (D).

The second study area is located in the Lockatong Creek watershed, a tributary of the Delaware River in Hunterdon County, New Jersey (Figure 2C). Lockatong Creek surface waters flow generally from north to south through an elevation-derived area of 62.33 km^2. The minimum elevation value in this watershed is 20.32 m and the maximum elevation value is 211.31 m. The upper part of the watershed landscape consists of cultivated crops and pasture interspersed with deciduous forests, and the lower part of the watershed consists mainly of deciduous forests with some cultivated crops and pasture.

The third study area is located in the Jacobs Creek watershed in Mercer County, New Jersey (Figure 2D). Jacobs Creek surface waters flow generally from north to south through an elevation-derived area of 34.28 km^2. The minimum elevation value in this watershed is 7.90 m and the maximum elevation value is 139.05 m. This watershed contains state and nationally designated historic districts and bridges that were impacted by flooding associated with Hurricane Irene (County of Mercer, 2011; Cusido, 2014). The landscape consists of both urban and commercial development with agriculture interspersed among forested areas.

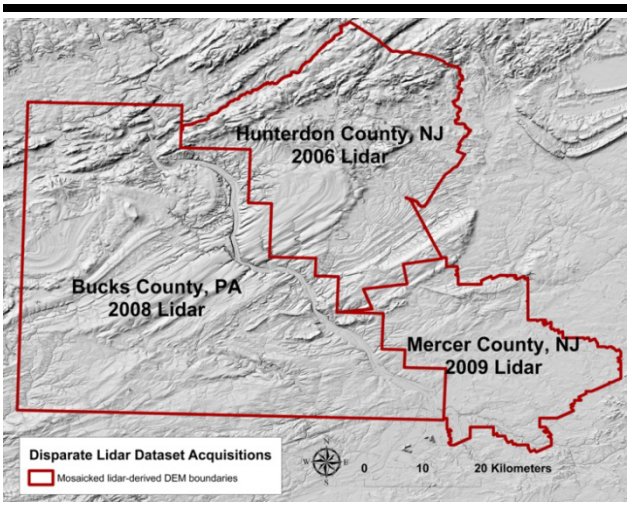

Figure 3. Map of disparate airborne lidar DEM datasets in New Jersey and Pennsylvania mosaicked as a high-resolution topographic DEM used to generate a hydrologically-corrected DEM.

Lidar Data Sources

Effective hydrologic modeling using lidar DEMs requires a single hydro-enforced surface model for the study area. Unfortunately, the extents of topographic data acquisitions are typically based on political boundaries such as county or state boundaries rather than watershed boundaries, and the most commonly delivered data are the traditional topographic DEMs (Poppenga *et al*., 2014a). Because the topographic DEMs were not hydrologically-corrected for hydrologic modeling, it was necessary to merge multiple topographic DEMs from disparate sources into a single surface prior to hydro-enforcement in the study areas.

For a part of the Delaware River watershed in New Jersey and Pennsylvania, three disparate airborne lidar datasets collected between 2006 and 2009 were obtained from the USGS. Because the lidar datasets were collected in various projections and at different time periods, a final mosaicked DEM was processed into one projection as Universal Transverse Mercator (UTM) Zone 18N, North American Datum of 1983 (NAD83), and North American Vertical Datum of 1988 (NAVD88) (Figure 3). The resulting 1-m resolution, 23-gigabyte mosaicked lidar DEM was used as the foundation layer for hydro-enforcement (Poppenga *et al*, 2014a). The metadata regarding each lidar dataset is provided in Table 1.

Field-Surveyed Culvert and Bridge Data Sources

Field-surveyed culvert and bridge datasets were obtained from public agencies in Pennsylvania and New Jersey (Table 2). Obtaining these datasets was a time-consuming process that consisted of contacting each public agency by email or phone to request various field survey data, and at times requiring signed agreements. Most drainage structure datasets obtained from the public agencies were in geographic information system (GIS) format; however, a few datasets were only available in spreadsheet or text format, thus necessitating a conversion to georeferenced coordinates. Table 3 lists the numerous data types and sources, sizes, maintenance, and ownership of the field-surveyed data that were obtained. All disparate culvert and bridge data were combined into one georeferenced dataset for the assessment analysis.

Field-surveyed metadata did not accompany the drainage structure datasets received from public agencies. Therefore, positional accuracy of the drainage structure locations were undetermined.

Digital Orthophoto Quadrangles Sources

Additional ancillary data used in this hydro-enforcement assessment included DOQs acquired by various vendors that were available from the USGS. Bucks County, Pennsylvania, DOQs were acquired by Aero Metric, Inc. (2010) on flight dates spanning from March 2010 to April 2010. Hunterdon County, New Jersey, DOQs were acquired by Photo Science, Inc. (2012a) on flight dates spanning from March 2012 to April 2012. Mercer County, New Jersey, DOQs were acquired by Photo Science, Inc. (2012b) on flight dates spanning from March 2012 to April 2012. The data consisted of 0.3-m pixel resolution (~1-ft), natural color orthoimages (Table 4).

In addition to merging multiple, disparate lidar DEMs into a single surface, it was also beneficial to merge the DOQs into one orthoimagery surface as well. This allowed seamless movement throughout a GIS environment during the hydro-enforcement assessments.

Table 1. *Lidar source data and digital elevation model (DEM) metadata that were used to generate the mosaicked DEM in the Delaware River Basin.*

Delaware River Basin Study Areas	Lidar Data Vendor	Lidar Data Acquisition Beginning and Ending Dates	Lidar Sensor	Projected Coordinate System	Horizontal and Vertical Datum	Fundamental Vertical Accuracy at 95% Confidence Level	Vendor Digital Elevation Model
Tinicum Creek, Bucks County, Pennsylvania	PAMAP Program, Bureau of Topographic and Geologic Survey, Pennsylvania Department of Conservation and Natural Resources (2008)	3/30/08 4/18/08	Not reported by vendor	Pennsylvania State Plane South (feet)	NAD83 NAVD88	24.5 cm	1-m horizontal resolution (model key points only) 1-m DEM regenerated from the bare earth lidar points
Lockatong Creek, Hunterdon County, New Jersey	EarthData International (2006)	9/20/06 9/21/06	Leica ALS-50	New Jersey State Plane (feet)	NAD83 NAVD88	36.3 cm	3-m horizontal resolution DEM reprocessed to 1-m horizontal resolution
Jacobs Creek, Mercer County, New Jersey	Photo Science, Inc. (2009)	3/31/09 4/25/09	Leica ALS50II	New Jersey State Plane (feet)	NAD83 NAVD88	35.3 cm	1-m horizontal resolution
Mosaicked Digital Elevation Model	See above rows	See above rows	See above rows	UTM Zone 18N	NAD83 NAVD88	See above rows	1-m horizontal resolution (23 gigabytes)

Table 2. *Surveyed culvert and bridge coordinate data obtained from public agencies.*

Delaware River Basin Counties	Surveyed Culvert or Bridge Data Source	Culvert or Bridge Type(s)
Bucks County, Pennsylvania	Bucks County, Doylestown, Pennsylvania and Pennsylvania Department of Transportation Bureau of Planning and Research Geographic Information Division, Harrisburg, Pennsylvania; National Bridges Inventory; U.S. Department of Transportation Bureau of Transportation Statistics	Commonwealth (State), County, Township, and City (borough) owned culverts and bridges; Compilation of bridge data supplied by the States to Federal Highway Administration for bridges located on public roads
Hunterdon County, New Jersey	Hunterdon County, Flemington, New Jersey; New Jersey Department of Transportation, Trenton, New Jersey; National Bridges Inventory; U.S. Department of Transportation Bureau of Transportation Statistics	County owned bridges and culverts; State owned bridges; Compilation of bridge data supplied by the States to Federal Highway Administration for bridges located on public roads
Mercer County, New Jersey	Mercer County, Transportation Asset Management Information Systems; Mercer County Department of Transportation and Infrastructure, Ewing, New Jersey; New Jersey Department of Transportation, Trenton, New Jersey; National Bridges Inventory; U.S. Department of Transportation Bureau of Transportation Statistics	State and County owned culverts and bridges; State owned bridges; Compilation of bridge data supplied by the States to Federal Highway Administration for bridges located on public roads

Table 3. *Surveyed culvert and bridge source data and ownership in the Delaware River Basin study areas.*

Surveyed Data Type (Sizes vary from < 5 ft; 5 ft – 20 ft; >= 20 ft)	Surveyed Entity Source Type	Maintenance or Ownership
Bridges	County	Government or private entities
Bridges	Department of Transportation	County or private entities
Bridges	Department of Transportation	State
Bridges/Culverts	Department of Transportation	County
Bridges/Culverts	County	County
Bridges/Culverts	County	Private entities
Bridges/Culverts	Department of Transportation	Private entities
Local Bridges	Department of Transportation	County
Commonwealth Bridges/Culverts	Department of Transportation	County
Suspect structures (not verified)	County	County

Table 4. *Digital orthophoto quadrangles (DOQs) source metadata for the study areas in the Delaware River Basin.*

Delaware River Basin Study Areas	DOQ Vendor	Flight Beginning and Ending Dates	Projected Coordinate System and Datum	Pixel Resolution (m)	Type of Imagery
Tinicum Creek, Bucks County, Pennsylvania	Aero Metric, Inc.	03/2010 04/2010	UTM Zone 18N (NAD83) or Pennsylvania State Plane South (ft)	0.3 (~1 ft)	Natural color orthoimages
Lockatong Creek, Hunterdon County, New Jersey	Photo Science, Inc.	3/14/2012 4/16/2012	UTM Zone 18N (m) (NAD83) or New Jersey State Plane Survey (ft)	0.3 (~1 ft)	Natural color orthoimages
Jacobs Creek, Mercer County, New Jersey	Photo Science, Inc.	3/14/2012 4/16/2012	UTM Zone 18N (m) (NAD83) or New Jersey State Plane Survey (ft)	0.3 (~1 ft)	Natural color orthoimages

Hydrologic-Enforcement Methods

Summary information for the hydro-enforcement methods is given herein; additional details regarding the methodology can be found in Poppenga *et al* (2010; 2012; 2013; 2014a). A combination of filling depressions in the DEM (hydro-conditioning) and draining techniques (hydro-enforcement) (Poppenga *et al.*, 2010; 2012) was used to define road fill, railroad grade, and other elevated features that caused artificially pooled depressions to form upstream of drainage structures (culverts or bridges). The elevations of these features were digitally modified to achieve hydrologic connectivity in lidar DEMs.

In the Delaware River Basin study areas, the mosaicked bare-earth lidar DEM was hydro-conditioned, or filled, to facilitate cell-to-cell routing (Figure 4). A difference grid (referred to hereafter as DiffGrid) was then generated by calculating the residuals between the bare-earth (unfilled) lidar DEM and the hydro-conditioned (filled) lidar DEM using Equation 1 (Poppenga *et al.*, 2010):

$$\Delta_{i,j} = F_{i,j} - U_{i,j} \quad (1)$$

where Δ is the DiffGrid, F is the hydro-conditioned, filled DEM, U is the bare-earth, unfilled DEM, and the indices i and j denote grid cell (i,j).

Because the DiffGrid can contain millions of un-drained depressions, it was not plausible to manually inspect all of them; only a subset of DiffGrid depressions was suitable for draining. To address the large number of un-drained depressions, criteria were set to exclude small depressions that were not likely to impact surface changes by draining them. DiffGrid summary statistics including area, minimum, maximum, and sum (volume), were calculated for each of the remaining depressions. Note that the volume parameter is a sum of the DiffGrid and represents the volume filled for each depression. Empirical testing was then conducted using various DiffGrid area and sum (volume) parameters to define un-drained depression subsets that prevented surface flow connectivity. These subsets were overlain on DOQs to visually analyze if the un-drained depressions needed draining and to determine which parameters provided the most plausible DiffGrid subset for hydro-enforcement. The empirical testing was based upon the hypothesis that depressions in the study areas within the following parameters were a proxy for candidate depressions that should be considered for draining. The set of candidate depressions that should be considered for draining, D_c, based on empirically-determined thresholds for planimetric area and volume, were identified:

$$D_c = \{D \mid A_D \geq 700\ \mathrm{m}^2\ \wedge V_D \geq 500\ \mathrm{m}^3\} \quad (2)$$

where D_c denotes candidate depressions, A_D denotes planimetric area, and V_D denotes volume.

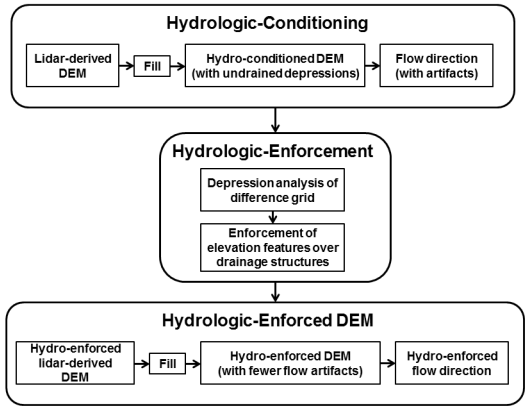

Figure 4. An overview of the hydrologic-conditioning and hydrologic-enforcement methods applied to the mosaicked lidar DEM study areas to obtain hydrologic connectivity. Detailed information regarding this methodology is provided in Poppenga *et al.* (2010; 2012).

Using the lidar DEM, the following hydro-enforcement methods were then executed for each location where depressions needed draining. A least cost path analysis was computed by calculating Euclidian distance between the lowest elevation value (source pixel) inside a depression location and the next lowest elevation value (target pixel) downstream of the raised elevation feature (Poppenga *et al.,* 2010; 2012; 2013). The calculated distance between the source and target pixels was used to extract a 1-pixel-wide transect DEM from the lidar

DEM. Because the transect DEM represented raised elevation values that artificially impede representative overland surface flow, the transect DEM values were lowered to equal that of the target pixel. The modified elevation values were mosaicked into a copy of the lidar DEM to preserve the topographic DEM while creating a hydrologically-corrected DEM (Figure 4). The hydro-enforcement process thereby creates monotonically decreasing elevation values in the hydrologically-corrected lidar DEM to achieve hydrologic connectivity. Note that the interactive part of the hydro-enforcement methodology is the selection of depressions that need draining. All other hydro-enforcement processes are automated.

Quantitative Assessments

This section describes the methods used to compare spatial correspondence between semi-automated hydro-enforcement and ancillary vector drainage structure data and DOQs.

Corresponding Field-Surveyed Drainage Structure Coordinates and Hydro-Enforced Transects

This quantitative assessment is a distance-based error metric defined between the lidar-derived hydro-enforced transect and a corresponding ancillary drainage structure. Because of the absence of hydrologic benchmarks that would be viable for hydro-enforcement assessments (Chow, 2010), field-surveyed culverts and bridges vector data that were obtained from numerous public agencies were used as reference points to assess the hydro-enforced transects (Tables 2 and 3). Because the field-surveyed datasets were a plethora of spatial coordinates collected on various dates by various entities with differing equipment, some hydro-enforced transects were near more than one set of field-surveyed coordinates. To eliminate redundant coordinates for any one hydro-enforced transect, the field-surveyed point data were compared with ancillary DOQs. If there were more than one set of spatial coordinates for any specific hydro-enforced transect, the coordinate that was nearest to the culvert or bridge identified in the DOQ was selected, and any duplicate coordinates near that location were eliminated.

A proximity analysis was conducted by defining corresponding relationships between each ancillary field-surveyed coordinates and their nearest hydro-enforced transect. The offset distance between each set of field-surveyed coordinates that corresponded with each hydro enforced transect was measured. These measurements were used to assess the hydro-enforcement techniques used in the Delaware River Basin study areas.

Corresponding Aerial Photograph Interpreted Drainage Structures and Hydro-Enforced Transects

In lidar DEMs, depressions do not always form near roads, where field-surveyed drainage structures are typically collected. Therefore, a merged dataset of disparate field-surveyed coordinates was not comprehensive enough to correspond with all DiffGrid depressions. A different approach was developed to define drainage structure reference points by interpreting DOQ aerial photographs in a GIS environment. This interpretation was conducted exclusively with DOQs and no other elevation or ancillary data.

The DOQs were interpreted to create points for culverts and bridges that were near each depression that was selected to hydro-enforce. Each interpreted point represented the center most point between the inlet and outlet of a drainage structure. Culvert locations were identified by having a visible inlet and outlet with vegetation often surrounding the road and culvert openings. Bridges were identified along larger streams and had rectangular features adjacent to the road sometimes with shadows below the bridge deck. Bridge decks often had contrasting brightness compared to the adjacent roads. At times, it was not possible to classify the drainage structure as a culvert or bridge, but an interpreted point was designated nevertheless because there were clearly defined stream channels on both sides of the impoundment. The drainage structure points interpreted from DOQs were used to define offset distances with hydro-enforced transects. The purpose of the assessment between DOQ-interpreted drainage structures and hydro-enforced transects was to identify additional reference points for validating hydro-enforcement.

RESULTS

Two different quantitative assessments were conducted in the study areas to evaluate hydro-enforcement of lidar DEMs. The first assessment analyzed the offset distances between the predicted hydro-enforced transects and the observed field-surveyed drainage structures (culverts/bridges) obtained from various public agencies. The second assessment analyzed the offset distances between the predicted hydro-enforced transects and the observed DOQ-interpreted drainage structures. It is worth clarifying here that the predicted hydro-enforced transects are drainage structure (culvert/bridge) locations where elevations were digitally adjusted in the hydrologically-corrected DEM to drain artificially pooled depressions to achieve hydrologic connectivity.

First Assessment Using Field-Surveyed Drainage Structure Coordinates

The number of ancillary field-surveyed drainage structures that corresponded with hydro-enforced transects was limited in all three study areas. For example, in Table 5, Column 2, although there were 33 artificially pooled depressions that needed hydro-enforcement in the Tinicum Creek study area, only five field-surveyed drainage structures corresponded to hydro-enforced transects (Column 3). This limited corresponding trend continued in the Lockatong Creek watershed where only 13 field-surveyed drainage structures corresponded with 39 hydro-enforced transects, and in the Jacobs Creek watershed where only 10 field-surveyed drainage structures corresponded to 49 hydro-enforced transects (Table 5). However, where there was a match between the predicted hydro-enforced transects and the observed field-surveyed data, the weighted mean offset distance was 3.91 m with a maximum distance of 28.61 m (Table 6). The 95th percentile ranking of the offset distance for Tinicum Creek was 3.53 m; Lockatong Creek was 18.13 m; and Jacobs Creek was 6.17 m (Table 6). Although these summary statistics imply successful hydro-enforcement where correspondence existed, the sample size of field-surveyed data was not sufficient in all three watersheds to derive a valid quantitative assessment (Table 5). An analysis was needed to determine the causes of the limited corresponding trend.

One cause of limited correspondence between hydro-enforced transects and field-surveyed data was removal (by the lidar data vendors) of elevation data representing bridge decks. In topographic DEM processing, bridge deck elevations are typically removed to obtain the bare-earth topographic surface.

Thus, a DiffGrid depression will not form in bridge deck locations where the lidar DEM has essentially been hydrologically-corrected. Although this may be an ideal situation for deriving monotonic surface flow, bridge deck removal had a negative effect in this hydro-enforcement assessment. Comparing a field-surveyed bridge coordinate with a DiffGrid depression that did not exist resulted in a limited correspondence. To compound this issue, the bridge removal process was not consistent in all study areas. Therefore, field-surveyed data were excluded in locations where bridge decks were removed from the lidar DEM. This issue did not apply to underground culvert drainage structures.

Table 5. *Comparison of hydro-enforced transects with ancillary field-surveyed drainage structures from public agencies.*

Delaware River Basin Study Areas	Hydro-Enforced Transects	Field-Surveyed Drainage Structures That Corresponded With Hydro-Enforced Transects	Offset Distance Between Field-Surveyed Drainage Structures and Hydro-Enforced Transects	
			Distance (m)	Number of Surveyed Drainage Structures
Tinicum Creek	33	5	<1	2
			>=1 & <3	1
			>=3 & <5	2
Lockatong Creek	39	13	<1	3
			>=1 & <3	5
			>=3 & <5	1
			>=5 & <10	1
			>=10 & <20	2
			>=20	1
Jacobs Creek	49	10	<1	3
			>=1 & <3	2
			>=3 & <5	3
			>=5 & <10	2

Table 6. *Summary statistics for offset distances between field-surveyed drainage structures and hydro-enforced transects.*

Delaware River Basin watersheds	Count	Min (m)	Max (m)	Mean (m)	Std. Dev. (m)	Median (m)	95th Percentile Ranking (m)
Tinicum Creek	5	0.076	3.545	2.025	1.646	2.52	3.534
Lockatong Creek	13	0.186	28.614	5.453	7.873	2.09	18.133
Jacobs Creek	10	0.190	6.399	2.840	2.320	2.33	6.169
All watersheds				3.908 Weighted Mean			

Temporal differences also caused limited correspondence between hydro-enforced transects and field-surveyed drainage structures. For example, newly constructed culverts or bridges that were not included in the field-surveyed datasets but appear in lidar DEMs will not correspond with hydro-enforced transects. Additionally, the plethora of collection methods and equipment accuracies may have contributed to the limited corresponding trend.

Combining disparate field-surveyed drainage structures into one dataset revealed that some watersheds contained more bridge coordinates than culvert coordinates. This issue surfaced in the Tinicum Creek watershed (Figure 2B) where only five field-surveyed drainage structures corresponded with the hydro-enforced transects (Table 5). Because most bridge decks in this watershed were already removed from the lidar DEM, the field-surveyed bridge coordinates were also removed from this assessment. The remaining few culvert coordinates did not correspond with the numerous DiffGrid depressions in the lidar DEM. The result was a limited correspondence in this watershed.

The parameters defined in the Methods section were used to select depressions that needed hydro-enforcing in the study areas. The purpose of the parameters was to reduce the

unreasonably high number of DiffGrid depressions to a manageable size so that hydro-enforcement processes could be executed. If the parameters were set too low, the results contained depressions (noise) that did not need hydro-enforcement. If the parameters were set too high, small depressions in need of hydro-enforcement were excluded from the selection. This resulted in errors because some smaller depressions were near culvert locations that actually corresponded to a field-surveyed drainage structure. This scenario is virtually impossible to predict until after hydro-enforcement results are reviewed.

Because of the extreme detail in the mosaicked lidar DEM, the number of DiffGrid depressions defined by the criteria that needed hydro-enforcement greatly exceeded the number of ancillary field-surveyed drainage structures. This was because DiffGrid depressions form not only near elevated road surfaces where culverts and bridges are field-surveyed but also near other features, such as dams, weirs, private drives, and bike path structures where public agencies may not have collected coordinates for drainage structures. Because of the complex nature of lidar DEMs, there will always be depressions in need of hydro-enforcement in locations other than elevated road features. Some DiffGrid depressions were located in the middle of land sections or in remote areas and did not correspond to any field-surveyed data. Therefore, because bridge and culvert coordinates are typically surveyed on roads, dependence upon the disparate field-surveyed datasets for hydro-enforcement validation resulted in an incomplete assessment.

Second Assessment Using Aerial Photograph Interpreted Drainage Structures

Due to the limited sample size between the predicted hydro-enforced transects and the observed data field-surveyed drainage structures (Table 5), an additional survey of aerial photograph-interpreted culverts and bridges from DOQs was developed to define drainage structures that were impounded in locations other than elevated road surfaces. This assessment, conducted exclusively with DOQs, was feasible for the project timeframe rather than conducting field surveys for the numerous depressions in the study areas.

The DOQ-interpreted assessment resulted in a greater number of corresponding drainage structures (Table 7, Column 3) than the field-surveyed data assessment (Table 5, Column 3). For example, in Tinicum Creek, there was a match between 26 air photograph-interpreted drainage structures and hydro-enforced transects (Table 7, Column 3), whereas there were only 5 matches with the field-surveyed data (Table 5, Column 3). A few drainage structures could not be confidently interpreted in the orthoimagery because of leaf-on conditions, especially in heavily vegetated areas surrounding the drainage structure. Additionally, the size of smaller drainage structures made it challenging to discern an inlet or outlet in the DOQs.

Table 7. *Comparison of hydro-enforced transects with air photograph-interpreted drainage structures from orthoimagery.*

Delaware River Basin Study Areas	Hydro-Enforced Transects	Air Photograph-Interpreted Drainage Structures That Corresponded With Hydro-Enforced Transects	Offset Distance Between Air Photograph-Interpreted Drainage Structures and Hydro-Enforced Transects	
Tinicum Creek	33	26	Distance (m)	Number of Surveyed Drainage Structures
			<1	8
			>=1 & <3	10
			>=3 & <5	4
			>=5 & <10	3
			>=10 & <20	1
Lockatong Creek	39	33	<1	7
			>=1 & <3	8
			>=3 & <5	3
			>=5 & <10	3
			>=10 & <20	6
			>=20	6
Jacobs Creek	49	35	<1	9
			>=1 & <3	9
			>=3 & <5	2
			>=5 & <10	10
			>=10 & <20	3
			>=20	2

Table 8. *Summary statistics for offset distances between air photograph-interpreted drainage structures and hydro-enforced transects.*

Delaware River Basin watersheds	Count	Min (m)	Max (m)	Mean (m)	Std. Dev. (m)	Median (m)	95th Percentile Ranking (m)
Tinicum Creek	26	0.159	12.453	2.690	2.673	2.009	6.844
Lockatong Creek	33	0.078	70.607	10.319	14.826	4.574	33.255
Jacobs Creek	35	0.201	45.633	6.302	9.053	2.879	20.007
All watersheds				6.713 Weighted Mean			

Although the DOQ-interpreted drainage structure assessment resulted in more matches with the hydro-enforced transects (Table 7, Column 3), the weighted mean offset distance was slightly higher (6.71 m) (Table 8) than the field-surveyed weighted mean offset distance (3.91 m) (Table 6). The maximum offset distance also increased for the interpreted data to 70.607 m (Table 8), while the field-surveyed maximum offset distance was 28.614 m (Table 6).

Because of these increases, the spread of offset distances, as illustrated in the box plots shown in Figure 5, was examined. The bottom of each plot is the 25th percentile and the top is the 75th percentile. Extreme offset values exceeding 1.5 times the interquartile range (25–75) are plotted as blue crosshairs. The median values are shown as horizontal red lines. The values along the vertical axis are the offset distances in meters. The characteristics for Lockatong Creek and Jacobs Creek display extreme offset distances while Tinicum Creek has good agreement. Further examination of the air photograph-interpreted data showed that the extreme offset distances were due to detention basin depressions that were impounded by features other than elevated road surfaces. Ironically, detention basin coordinates were usually not available in the field-surveyed data. However, because the detention basin points were interpreted in the orthoimagery, they caused extreme offset distances in this second hydro-enforcement assessment.

There are a variety of detention basin outlet structure types. For the most part, those identified were discharge stand pipe or culvert points in the orthoimagery that corresponded with DiffGrid depressions that were selected to drain. At times, it was not clear in the orthoimagery if the detention basin structure drained overland or sub-surface. The impounding feature (berm) and the stand pipe or culvert was visible, yet the downstream drainage was not evident in the imagery. For sub-surface drainage, if a detention basin discharge point was designated, the result was an extreme offset distance. This was because hydro-enforcement, initiated at the lowest point in the detection basin (usually an outlet point), generated a lengthy transect when searching for a nearby channel to drain downstream. In some of the detention basins the lowest elevation was not located near a stand pipe or culvert; perhaps this was because detention basins are designed to impound water for a short duration, or perhaps this was due to bare-earth processing errors in heavily vegetated areas. Regardless of the cause, the result was also an extreme offset distance between the interpreted points and the hydro-enforced transects. Therefore, detention basin depressions and their corresponding interpreted points needed to be removed from this second assessment to avoid degrading the lidar DEM with long hydro-enforced transects.

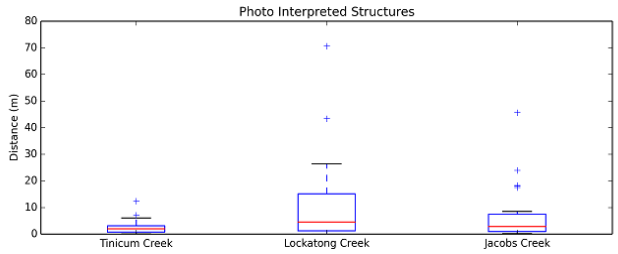

Figure 5. Box-and-whisker plot of the distance between air photograph-interpreted drainage structures and hydro-enforced transects in the three Delaware River study area watersheds.

Summary statistics and percentile rankings for remaining DOQ-interpreted points exclusive of detention basin outlet structure points were then re-calculated. The weighted mean offset distance improved from 6.71 m (Table 8) to 4.94 m (Table 9). The results in Table 9 show an improved corresponding agreement between interpreted points and hydro-enforced transects, particularly in the Lockatong Creek watershed (Figure 6). The cumulative percent graphs, shown in Figure 7, illustrate that 95% of the offset distances were less than 7.04 m in Tinicum Creek, 21.69 m in Lockatong Creek, and 10.44 m in Jacobs Creek (Table 9).

In general, the variability of hydro-enforcement assessment results in the Lockatong Creek and Jacobs Creek watersheds was most likely caused by bare-earth processing, or in other words the failure to remove lidar points classified as vegetation. Additionally, in vegetated areas, as well as in some channels, elevation errors appeared in the DEM, thereby causing extreme offset distances in the hydro-enforcement assessments. Perhaps these errors occurred because of insufficient lidar points in specific areas during DEM generation and artifacts from natural neighbor resampling.

Table 9. *Summary statistics for offset distance between air photograph-interpreted data excluding detention basins and hydro-enforced transects.*

Delaware River Basin watersheds	Count	Min (m)	Max (m)	Mean (m)	Std. Dev. (m)	Median (m)	95th Percentile Ranking (m)
Tinicum Creek	22	0.159	12.453	3.027	2.766	2.30	7.044
Lockatong Creek	20	0.078	26.481	6.70	7.749	4.180	21.685
Jacobs Creek	20	0.201	45.633	5.29	9.91	2.437	10.441
All watersheds				4.942 Weighted Mean			

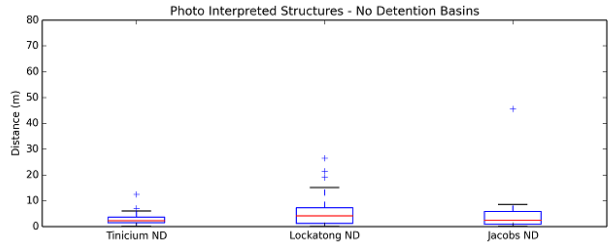

Figure 6. Box-and-whisker plot of the distance between air photograph-interpreted drainage structures and hydro-enforced transects excluding detention basin depressions in the three Delaware River study area watersheds. ND = no detention basins.

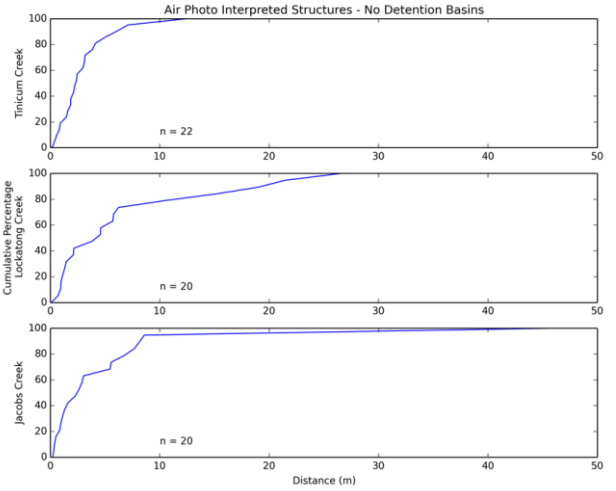

Figure 7. Cumulative percentage graphs (excluding detention basins) of the distance between air photograph-interpreted drainage structures and hydro-enforced transects in the three Delaware River study area watersheds.

DISCUSSION

Three discussion points compose this part of the article. The first point explains how the hydro-enforcement assessment objective was not plausible due to limited correspondence between hydro-enforced transects and field-surveyed data. This problem led to the development of a second hydro-enforcement assessment. Next, the importance of an in-depth review of the DiffGrid in all study areas to achieve portability of the hydro-enforcement methods is explained. Finally, future research on frequency distributions that could improve upon the published hydro-enforcement methods (Poppenga *et al.*, 2010) is described.

Hydro-enforcement validation proved challenging because of the lack of comprehensive hydrologic benchmarks that could be referenced as ground-truth for drainage structures (culverts/bridges). Thus, the initial objective was to obtain field-surveyed culvert and bridge coordinates from various public agencies to use as reference points to compare with hydro-enforced transects. Addressing that objective led to several problems, including discovery of duplicative field-surveyed coordinates near some depressions, missing field-surveyed data in remote locations, inconsistent removal of bridge elevations in the lidar DEM, and the lack of culvert data for small drainage areas. These problems resulted in limited correspondence between hydro-enforced transects and field-surveyed data, and an inadequate sample size to conduct a viable assessment.

Limited correspondence (matches) between hydro-enforced transects and field-surveyed data does not necessarily imply that hydro-enforcement is not a viable solution for obtaining hydrologic connectivity, nor does it imply that ancillary field-surveyed datasets are incorrectly collected. It simply means that a more comprehensive field-surveyed dataset was needed to assess artificially pooled depressions that did not form near road features. Because there are always more depressions that need draining than available ancillary reference point data, a quantitative assessment of hydro-enforcement required a different approach. Therefore, a second hydro-enforcement assessment was developed where DOQ-interpreted drainage structures near each depression were used as reference points to compare with hydro-enforced transects. Considering the project timeframe, this assessment proved more viable than individually collecting field coordinates for each of the numerous depressions in need of draining.

The hydro-enforcement methods assessed in this article (Poppenga *et al.*, 2010; 2012) are transferable to other geographic areas. However, because the landscapes of different geographic areas are variable, empirical testing of basic DiffGrid attributes, such as Area or Sum (Volume), is suggested for each study area to define parameters that threshold the millions of depressions to a manageable subset that impact hydrologic connectivity. Note that the quality of the DiffGrid depressions is based upon the accuracy of the bare-earth lidar point classification and the derivative lidar DEM. In other words, the more accurate the bare-earth classified lidar points the more reliable the bare-earth lidar DEM is for conducting

hydro-enforcement. If lidar DEMs are poorly classified as bare-earth in vegetated areas or if the wrong re-sampling algorithm is used during DEM generation, there will be artifacts in the DEM, and the hydro-enforcement logic, as assessed in this article, will not function as designed.

Additional research on frequency distributions may provide insight into automated or semi-automated depression selection for hydro-enforcement. For example, the three-dimensional shape of each depression provides metrics that could be used as proxies to determine the likelihood that a depression could be drained or not drained. Figure 8 illustrates a depression with a flat bottom that extends over most of the area. The histogram shows the depth frequencies shifted to the lower depths of the depression. These types of depressions typically do not exhibit a single, lowest drainage location where a drainage structure would be located. However, these metrics may be an indicator to categorize depressions as drainable or non-drainable. Conversely, the depression depicted in Figure 9 shows the deepest part (dark red) located near the left perimeter of the depression. In this example, the histogram is shifted to the shallow depths of the depression and very few cells are located at the deepest location. There is more topographic relief in this depression, which has a maximum depth of 12.6 m. Therefore, these types of depressions exhibit a single location at the lowest point and can be considered as drainable depressions using the hydro-enforcement methods discussed in this article. Using these three-dimensional shape metrics in conjunction with other topographic signatures may improve the efficiency for selecting depressions for hydro-enforcement.

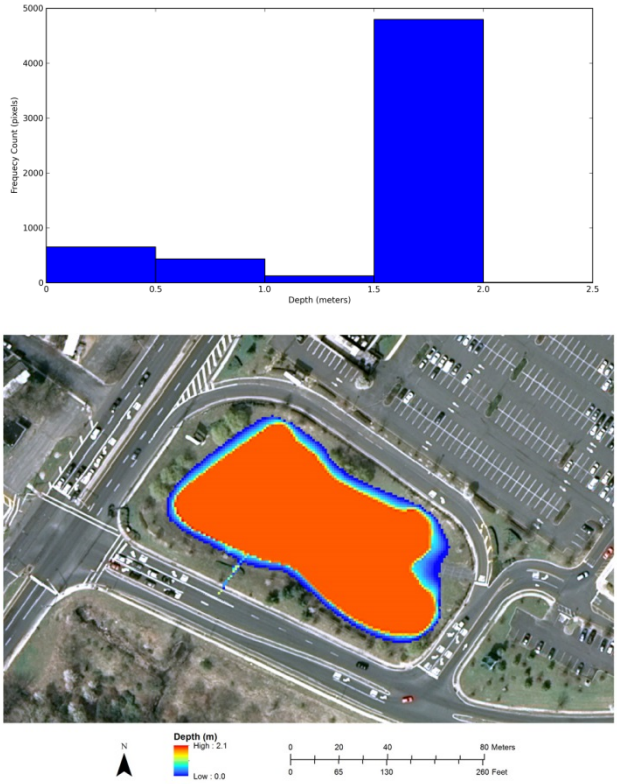

Figure 8. Histogram and difference grid of a shallow depression that is not hydrologically-enforced (drained).

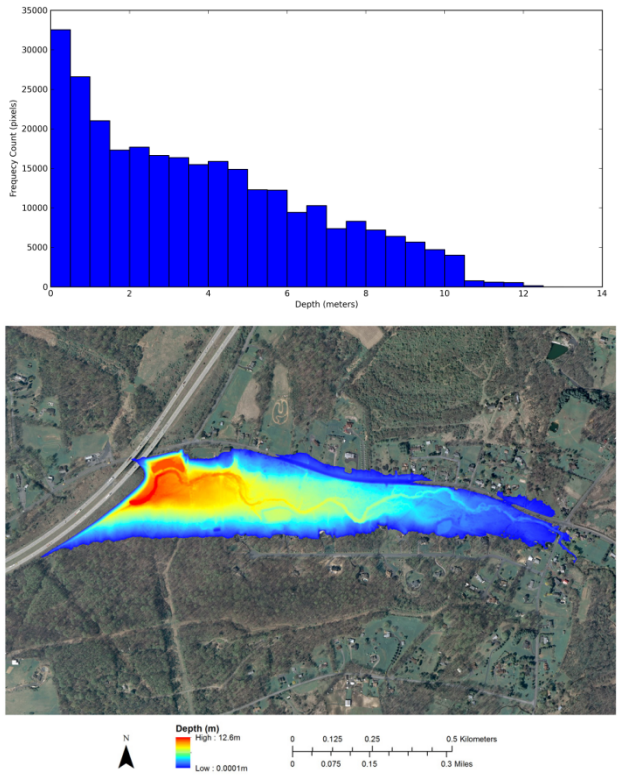

Figure 9. Histogram and difference grid of a depression that can be hydrologically-enforced (drained).

CONCLUSION

Hydrologic connectivity of lidar elevation surfaces is critical to understanding constantly changing coastal landscapes; however, unless hydro-enforced, drainage structures used to control flow on the landscape are missed and can cause incorrect overland surface flow to coastal waters. Because highly detailed lidar elevation data include features such as bridge decks and road fill overlying culverts, artificially pooled depressions that form upstream of drainage structures impede modeled overland surface flow. Although elevation surfaces are often processed to remove these types of features, the degree to which this is done varies greatly. In this article, digital methods for hydro-enforcing bridge deck and road fill elevations and other depressions not located near roads are presented to eliminate the impacts of constructed features on represented surface flow.

The hydro-enforcement methods presented in this article are a relatively different approach for achieving hydrologic connectivity; therefore, validation assessments were conducted

by determining the residuals between predicted hydro-enforced transects and observed ancillary drainage structure data. This type of validation has rarely been employed in the published literature; therefore, an innovative approach was developed for conducting hydro-enforcement assessments. Initially ancillary field-surveyed data obtained from public agencies were compared with hydro-enforced transects. However, many artificially pooled depressions in lidar DEMs are not impounded near road features where field-surveyed data are typically collected; therefore, field-surveyed drainage structures were not a comprehensive solution for conducting a quantitative assessment of hydro-enforcement. An interpretation of digital orthophoto quadrangles (orthoimagery) was a more complete approach to validating hydrologic connectivity obtained through hydro-enforcement.

The concept of hydrologic connectivity is important when using lidar elevation data for evaluating natural disaster impacts and potential climate change risks. As such, hydro-enforced elevation data (land elevation) can be integrated with bathymetric (water depth) datasets to generate seamless cross-shoreline topobathymetric datasets (Danielson *et al.*, 2013) that can be incorporated into the Coastal National Elevation Database (CoNED) Applications Project (Poppenga *et al.*, 2014a). The result is an enhanced DEM that can be used as a base layer in hydrologic models to more accurately and realistically represent overland flow. By merging lidar hydro-enforced land elevation and bathymetric data, a three-dimensional topographic/bathymetric, or topobathymetric, seamless cross-shoreline surface can be developed to analyze topographic and structural features along the land/water interface. Hydro-enforced topobathymetric data are useful for water inundation mapping and hydrodynamic modeling, climate change studies of coastal sea-level rise in vulnerable land/water interfaces along coastal zones, and other Earth science applications, such as the development of sediment-transport, debris flow modeling, and storm surge models.

ACKNOWLEDGMENTS

This work was supported by the U.S. Geological Survey (USGS) Climate and Land Use Mission Area, Research and Development Program and the USGS Natural Hazards Mission Area, Coastal and Marine Geology Program (CMGP). The research reported here is part of a larger USGS effort, the Coastal National Elevation Database (CoNED) Applications Project, a multi-year project funded by the USGS CMGP. The contributions of the following individuals are gratefully acknowledged: John Brock and Jeff Danielson (USGS) for development of the CoNED Applications Project, and Dean Gesch (USGS) for his scientific advice. The authors also thank the journal reviewers and Christopher Parrish for suggestions that improved the manuscript. The authors are grateful to Mercer and Hunterdon Counties, New Jersey, and the City of Trenton, New Jersey; New Jersey Department of Transportation; Pennsylvania Department of Transportation; Bucks County, Pennsylvania, and the U.S. Department of Transportation, Federal Highway Administration, Bureau of Transportation Statistics for access to their field-surveyed data. Work by Bruce Worstell was performed under USGS contract G15PC00012.

Any use of trade, firm, or product names is for descriptive purposes only and does not imply endorsement by the U.S. Government.

LITERATURE CITED

Aero Metric, Inc., 2010. USGS High resolution orthoimagery for Bucks County, Pennsylvania, Sheboygan, WI. Data collection by Aero Metric, Inc. and distributed by USGS *The National Map*. Metadata available online at http://tdds.cr.usgs.gov/metadata/ortho/18T/VK/18TVK755700_201003_0x3000m_CL_1.htm.

ARCADIS U.S., Inc., 2011. *ADCIRC Based Storm Surge Analysis of Sea Level Rise in Grand Bay*. Arlington, Virginia: The Nature Conservancy, 84p.

Barber, C.P. and Shortridge, A.M., 2005. Terrain representation, scale, and hydrologic modeling: Does LiDAR make a difference? *Autocarto*, (Las Vegas, Nevada), March, 16p.

Brock, J. and Sallenger, A.H., 2001. *Airborne Topographic Lidar Mapping for Coastal Science and Resource Management*. *U.S. Geological Survey Open-File Report 2001–46*, 4p.

Brock, J.C. and Purkis, S.J., 2009. The emerging role of lidar remote sensing in coastal research and resource management. *In:* Brock, J.C. and Purkis, S.J. (eds.), *Coastal Applications of Airborne Lidar*. *Journal of Coastal Research*, Special Issue No. 53, pp. 1–5.

Burkett, V.R. and Davidson, M.A. (eds.), 2012. *Coastal Impacts, Adaptation and Vulnerability: A Technical Input to the 2013 National Climate Assessment*. Cooperative report to the 2013 National Climate Assessment, 150p.

Buxton, H.T.; Andersen, M.E.; Focazio, M.J.; Haines, J.W.; Hainly, R.A.; Hippe, D.J., and Sugarbaker, L.J., 2013. *Meeting the Science Needs of the Nation in the Wake of Hurricane Sandy—A U.S. Geological Survey Science Plan for Support of Restoration and Recovery. U.S. Geological Survey Circular 1390*, 26p.

Cho, H.; Kampa, K., and Slatton, K.C., 2007. Morphological segmentation of lidar digital elevation models to extract stream channels in forested terrain. *Proceedings of the 2007 IEEE International Geoscience and Remote Sensing Symposium (IGARSS '07)*, 2, pp. 3182–3185.

Cho, H-C.; Slatton, K.C.; Krekeler, C.R., and Cheung, S., 2011. Morphology-based approaches for detecting stream channels from ALSM data. *International Journal of Remote Sensing*, 32(24), 9571–9597.

Chow, T.E., 2010. An assessment of hydrologic enforcement methods on various drainage features. *GIScience*, *Sixth International Conference on Geographic Information Science* (Zurich, Switzerland).

County of Mercer, Department of Transportation & Infrastructure, 2011. *Letter to the Acting Administrator, New Jersey Department of Environmental Protection regarding Hurricane Irene Storm Damage*, September 8.

Cusido, C., 2014. Jacobs Creek Bridge weakened by Irene, set to move: *New Jersey On-Line*, September 13, 2011, http://webcache.googleusercontent.com/search?q=cache:http://www.nj.com/mercer/index.ssf/2011/09/jacobs_creek_bridge_weakened_b.html.

Danielson, J.J.; Brock, J.C.; Howard, D.M.; Gesch, D.B.;

Bonisteel-Cormier, J.M., and Travers, L.J., 2013. *Topobathymetric Model of Mobile Bay, Alabama. U.S. Geological Survey Data Series 769*, scale 1:55,000, 6 map sheets.

Delaware River Basin Commission. 2004. *Lower Delaware Monitoring Program: 2000-2003 Results and Water Quality Management Recommendations*. West Trenton, New Jersey: Delaware River Basin Commission, 46p.

Duke, G.; Kienzle, S.W.; Johnson, D., and Byrne, J., 2003. Improving overland flow routing by incorporating ancillary road data into digital elevation models. *Journal of Spatial Hydrology,* 3(2), 27.

EarthData International, 2006. *Hunterdon County, NJ, Aerial Lidar Mapping*. Frederick, Maryland: Data collected by EarthData International and distributed by Watershed Concepts, Charlotte, North Carolina.

Evans, G.A.; Danielson, J.J.; Tyler, D.J.; Barras, J.A., and Brock, J.C., 2014. Validation of the 3-meter topobathymetric elevation model for southern Louisiana. *Proceedings of the Association of American Geographers Annual Meeting* (Tampa, Florida).

Gesch, D.B., 2009. Analysis of lidar elevation data for improved identification and delineation of lands vulnerable to sea level rise. *In:* Brock, J.C. and Purkis, S.J. (eds.), *Coastal Applications of Airborne Lidar, Journal of Coastal Research,* Special Issue No. 53, pp. 49–58.

Gesch, D.B., 2013. Consideration of vertical uncertainty in elevation-based sea-level rise assessments: Mobile Bay, Alabama case study. *In:* Brock, J.C.; Barras, J.A., and Williams, S.J. (eds.), *Understanding and Predicting Change in the Coastal Ecosystems of the Northern Gulf of Mexico*. *Journal of Coastal Research*, Special Issue No. 63, pp. 197–210.

Gesch, D.B.; Gutierezz, B.T., and Gill, S.K., 2009. Coastal Elevations. *In:* Titus, J.G. (ed.), *Coastal Sensitivity to Sea level Rise: A Focus on the Mid-Atlantic Region.* Washington, D.C.: Environmental Protection Agency, pp. 25–42.

Gesch, D.B.; Oimoen, M.J., and Evans, G.A., 2014. *Accuracy Assessment of the U.S. Geological Survey National Elevation Dataset, and Comparison with Other Large-Area Elevation Datasets—SRTM and ASTER. U.S. Geological Survey Open-File Report, 2014–1008*, 10p.

Heidemann, H.K., 2012a, Digital elevation models. *In:* Renslow, M.S., (ed.), *Manual of Airborne Topographic Lidar*: Bethesda, Maryland: American Society for Photogrammetry and Remote Sensing, pp. 283–310.

Heidemann, H.K., 2012b, Existing standards and guidelines. *In:* Renslow, M.S., (ed.), *Manual of Airborne Topographic Lidar:* Bethesda, Maryland: American Society for Photogrammetry and Remote Sensing, pp. 250–277.

Heidemann, H.K., 2014, *Lidar base specification version 1.2 (November 2014): U.S. Geological Survey Techniques and Methods book 11*, chap. B4, 67 p.

Heistermann, M., and Kneis, D., 2011. Benchmarking quantitative precipitation estimation by conceptual rainfall-runoff modeling. *Water Resources Research*, 47(6), W06514.

Kenny, F. and Matthews, B., 2005. A methodology for aligning raster flow direction data with photogrammetrically mapped hydrology. *Computers & Geosciences*, 31(6), 768–779.

Leopold, L.B., 1962. *A National Network of Hydrologic Bench Marks: U.S. Geological Survey Circular 460–B*, 4p.

Li, X.; Rowley, R.J.; Kostelnick, J.C.; Braaten, D.; Meisel, J., and Hulbutta, K., 2009. GIS analysis of global impacts from sea-level rise. *Photogrammetric Engineering and Remote Sensing*, 75(7), 807–818.

MacDonald, T., 2012. Vulnerability and Impacts on Human Development. *In:* Burkett, V.R. and Davidson, M.A., (eds.), *Coastal Impacts, Adaptation, and Vulnerabilities: A Technical Input to the 2013 National Climate Assessment*. Washington, DC: National Oceanic and Atmospheric Administration, *National Climate Assessment Regional Technical Input Report Series*, pp. 66–97.

Mast, M.A. and Turk, J.T., 1999. *Environmental Characteristics and Water Quality of Hydrologic Benchmark Network Stations in the Midwestern United States, 1963–95. U.S. Geological Survey Circular 1173-B*, 130p.

Maune, D.F., 2007. Definitions, *In:* Maune, D.F., (ed.), *Digital Elevation Model Technologies and Applications—The DEM Users' Manual*, 2nd Edition. Bethesda, Maryland: American Society for Photogrammetry and Remote Sensing, pp. 550–551.

Maune, D.F.; Kopp, S.M.; Crawford, C.A., and Zervas, C.E., 2007. Introduction. *In:* Maune, D.F. (ed.), *Digital Elevation Model Technologies and Applications—The DEM Users Manual*, 2nd Edition. Bethesda, Maryland: American Society for Photogrammetry and Remote Sensing, pp. 1–35.

McMillan, H.; Krueger, T., and Freer, J., 2012. Benchmarking observational uncertainties for hydrology: Rainfall, river discharge and water quality. *Hydrological Processes*, 26, 4078–4111.

Medeiros, S.C., 2012. Incorporating Remotely Sensed Data into Coastal Hydrodynamic Models: Parameterization of Surface Roughness and Spatio-Temporal Validation of Inundated Area. Orlando, Florida: University of Central Florida, Ph.D. dissertation, 471p.

Medeiros, S.C.; Ali, T.A.; Hagen, S.C., and Raiford, J.P., 2011. Development of a seamless topographic bathymetric digital terrain model for Tampa Bay, Florida, *Photogrammetric Engineering & Remote Sensing*, 77(12), 1249–1256.

Murdoch, P.S.; McHale, M.R.; Mast, M.A., and Clow, D.W., 2005. *The U.S. Geological Survey Hydrologic Benchmark Network. USGS Fact Sheet 2005-3135*, 5p.

National Geodetic Survey, 2012. GPS on Bench Marks (GPSBM) GEOID12A: http://www.ngs.noaa.gov/GEOID/GEOID12A/GPSonBM12A.shtml.

National Park Service, 2012. Delaware River Basin National Wild and Scenic River Values, Pennsylvania, New York, and New Jersey, U.S. Department of the Interior. http://www.state.nj.us/drbc/library/documents/NPSreport_DRBwild-scenic-river-valuesSept2012.pdf.

NOAA, 2010. *Technical Considerations for Use of Geospatial Data in Sea Level Change Mapping and Assessment*. Silver Spring, Maryland: National Oceanic and Atmospheric Administration, National Ocean Service, *NOAA Technical Report NOS 2010–01*, 130p.

PAMAP Program, PA Department of Conservation and Natural Resources, Bureau of Topographic and Geologic Survey,

2008. PAMAP program 3.2 ft. digital elevation model of Pennsylvania. Data collected by PAMAP Program, Middletown, PA and distributed by Pennsylvania Spatial Data Access (PASDA), University Park, PA, and Penn State Center for Geographic Information Services, Middletown, PA.

Photo Science Inc., 2009. High density lidar data for Mercer County, NJ. Data collected by Photo Science Inc., Lexington, KY.

Photo Science, Inc., 2012a. USGS High resolution orthoimagery for Hunterdon County, New Jersey, Lexington, KY: Data collection by Photo Science, Inc. and distributed by USGS *The National Map*. Metadata available online at http://tdds.cr.usgs.gov/metadata/ortho/18T/WK/18TWK055700_201203_0x3000m_CL_1.htm.

Photo Science, Inc., 2012b. USGS High resolution orthoimagery for Mercer County, New Jersey, Lexington, KY: Data collection by Photo Science, Inc. and distributed by USGS *The National Map*. Metadata available online at http://tdds.cr.usgs.gov/metadata/ortho/18T/WK/18TWK115610_201203_0x3000m_CL_1.htm.

Poppenga, S.K.; Gesch, D.B., and Worstell, B.B., 2013. Hydrography change detection: The usefulness of surface channels derived from LiDAR DEMS for updating mapped hydrography. *Journal of the American Water Resources Association*, 49(2), 371–389.

Poppenga, S.K.; Worstell, B.B.; Danielson, J.J.; Brock, J.C.; Evans, G.A., and Heidemann, H.K., 2014a, *Hydrologic Enforcement of Lidar DEMs. U.S. Geological Survey Fact Sheet 2014–3051*, 4p.

Poppenga, S.K.; Worstell, B.B.; Evans, G.A.; Danielson, J.J.; Brock, J.C., and Heidemann, H.K., 2014b. Hydrologic-enforcement of lidar DEMs in select reaches of the Delaware River Basin. *Proceedings of the Association of American Geographers Annual Meeting* (Tampa, Florida).

Poppenga, S.K.; Worstell, B.B.; Stoker, J.M., and Greenlee, S.K., 2009, *Comparison of Surface Flow Features from Lidar-Derived Digital Elevation Models with Historical Elevation and Hydrography Data for Minnehaha County, South Dakota. U.S. Geological Survey Scientific Investigations Report 2009–5065*, 24 p.

Poppenga, S.K.; Worstell, B.B.; Stoker, J.M., and Greenlee, S.K., 2010. *Using Selective Drainage methods to Extract Continuous Surface Flow from 1-Meter Lidar-Derived Digital Elevation Data. U.S. Geological Survey Scientific Investigations Report, 2010–5059*, 12p.

Poppenga, S.K.; Worstell, B.B.; Stoker, J.M., and Greenlee, S.K., 2012. Using selective drainage methods to hydrologically-condition and hydrologically-enforce lidar-derived surface flow. *Proceedings, Remote Sensing and Hydrology 2010, IAHS Publication 352*, (Jackson Hole, Wyoming), pp. 329–332.

Poulter, B. and Halpin, P.N., 2008. Raster modelling of coastal flooding from sea-level rise. *International Journal of Geographical Information Science*, 22(2), 167–182.

Poulter, B.; Goodall, J.L., and Halpin, P.N., 2008. Applications of network analysis for adaptive management of artificial drainage systems in landscapes vulnerable to sea level rise. *Journal of Hydrology*, 357(3–4), 207–217.

Samsung L.; Thatcher, C.A.; Brock, J.C.; Kimbrow, D.R.; Danielson, J.J., and Reynolds, B.J., 2013. Accuracy assessment of a mobile terrestrial lidar survey at Padre Island National Seashore. *International Journal of Remote Sensing*, 34(18), 6355–6366.

Saunders, W.K., 2000. Preparation of DEMs for use in environmental modeling analysis. *In:* Maidment, D. and Djokic, D. (eds.), *Hydrologic and Hydraulic Modeling Support with Geographic Information Systems*. Redlands, California: ESRI Press, pp. 29–51.

Schmid, K.A.; Hadley, B.C., and Wijekoon, N., 2011. Vertical accuracy and use of topographic LIDAR data in coastal marshes. *Journal of Coastal Research*, 27(6A), 116–132.

Seibert, J., 2001. On the need for benchmarks in hydrological modelling. *Hydrological Processes*, 15(6), 1063–1064.

Sheets, J.; Brenner, J., and Gilmer, B., 2012. Assessing the potential impact of sea-level rise and climatic hazards on ecological and human communities within the Northern Gulf of Mexico. Arlington, Virginia: *The Nature Conservancy*, 34p.

Soille, P.; Vogt, J., and Colombo, R, 2003. Carving and adaptive drainage enforcement of grid digital elevation models. *Water Resources Research*, 39(12), 1366.

Stiff, D.; Hopkinson, C., and Webster, T., 2008. Preparing LiDAR data for river flood impact assessment in a GIS environment: A practical approach. *In:* Hopkinson, C.; Pietroniro, A., and Pomeroy, J.W. (eds.), *Hydroscan: Airborne Laser Mapping of Hydrological Features and Resources*. Ottawa, Canada: Canadian Water Resources Association, pp. 119–138.

Stoker, J.; Harding, D., and Parrish, J., 2008. The need for a National lidar dataset. *Photogrammetric Engineering & Remote Sensing*, 74(9), 1066–1068.

Stoker, J.M.; Tyler, D.J.; Turnipseed, D.P.; Van Wilson, K., Jr., and Oimoen, M.J., 2009. Integrating disparate lidar datasets for a regional storm tide inundation analysis of Hurricane Katrina. *In:* Brock, J.C. and Purkis, S.J. (eds.), *Coastal Applications of Airborne Lidar. Journal of Coastal Research*, Special Issue No. 53, pp. 66–72.

Thatcher, C.; Danielson, J.J.; Gesch, D.B., and Kimbrow, D., 2014. The use of GPS and terrestrial lidar data to evaluate the accuracy of bare earth airborne lidar in wetland habitats. *Proceedings of the Association of American Geographers Annual Meeting* (Tampa, Florida).

Turcotte, R.; Fortin, J.-P.; Rousseau, A.N.; Massicotte, S., and Villeneuve, J.-P., 2001. Determination of the drainage structure of a watershed using a digital elevation model and a digital river and lake network. *Journal of Hydrology*, 240(3–4), 225–242.

Turnipseed, D.P.; Wilson, K.V., Jr.; Stoker, J., and Tyler, D., 2007. Mapping hurricane Katrina peak storm surge in Alabama, Mississippi, and Louisiana. *Proceedings of the 37th Mississippi Water Resources Conference* (Jackson, Mississippi), pp. 202–207.

Webster, T. and Stiff, D., 2008. The prediction and mapping of coastal flood risk associated with storm surge events and long-term sea level changes. *In:* Brebbia, C.A. and Beriatos, E., (eds.), *Risk Analysis VI Simulations and Hazard Mitigation*. Southhampton, United Kingdom: WIT Press, pp.

129–138.

Webster, T.L. and Forbes, D.L., 2006. Airborne laser altimetry for predictive modelling of coastal storm-surge flooding. *In:* LeDrew, E. and Richardson, L. (eds.), *Remote Sensing of Aquatic Ecosystem Processes, Science and Management Applications*. Dordrecht, Netherlands: Springer, pp. 157–180.

Westerink, J.J.; Luettich, R.A.; Feyen, J.C.; Atkinson, J.H.; Dawson, C.; Roberts, H.J.; Powell, M.D.; Dunion, J.P.; Kubatko, E.J., and Pourtaheri, H., 2008. A basin- to channel-scale unstructured grid hurricane storm surge model applied to southern Louisiana. *Monthly Weather Review*, 136(3), 833–864.

Zhang, H. and Huang, G., 2009. Building channel networks for flat regions in digital elevation models. *Hydrological Processes*, 23(20), 2879–2887.

Zhang, K.; Dittmar, J.; Ross, M., and Bergh, C., 2011. Assessment of sea-level rise impacts on human population and real property in the Florida Keys. *Climatic Change*, 107(1), 129–146.